Designing hydrocolloid based food-ink formulations for extrusion 3D printing

Gholamipour-Shirazi, Azarmidokht; Norton, Ian T.; Mills, Tom

DOI:
10.1016/j.foodhyd.2019.04.011

Document Version
Peer reviewed version

Citation for published version (Harvard):
Gholamipour-Shirazi, A, Norton, IT & Mills, T 2019, 'Designing hydrocolloid based food-ink formulations for extrusion 3D printing', *Food Hydrocolloids*, vol. 95, pp. 161-167. https://doi.org/10.1016/j.foodhyd.2019.04.011

Accepted Manuscript

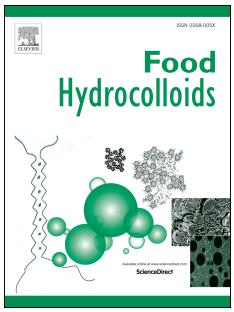

Designing hydrocolloid based food-ink formulations for extrusion 3D printing

Azarmidokht Gholamipour-Shirazi, Ian T. Norton, Tom Mills

PII: S0268-005X(18)32415-9

DOI: https://doi.org/10.1016/j.foodhyd.2019.04.011

Reference: FOOHYD 5040

To appear in: *Food Hydrocolloids*

Received Date: 17 December 2018

Revised Date: 20 March 2019

Accepted Date: 5 April 2019

Please cite this article as: Gholamipour-Shirazi, A., Norton, I.T., Mills, T., Designing hydrocolloid based food-ink formulations for extrusion 3D printing, *Food Hydrocolloids* (2019), doi: https://doi.org/10.1016/j.foodhyd.2019.04.011.

Graphical abstract

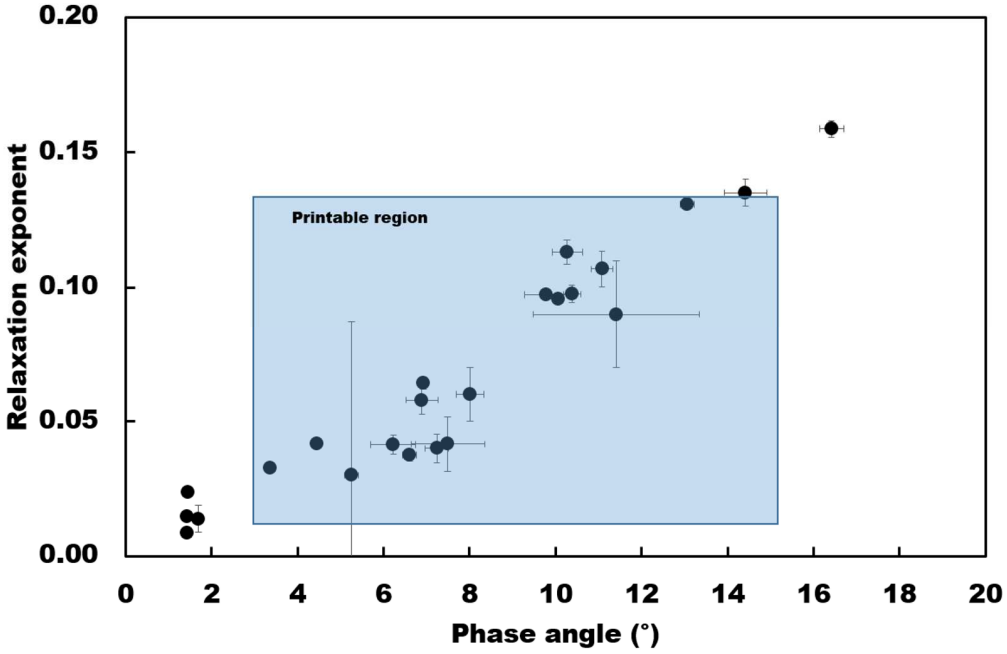

Designing Hydrocolloid Based Food-Ink Formulations for Extrusion 3D Printing

Azarmidokht Gholamipour-Shirazi *, Ian T. Norton, Tom Mills

Department of Chemical Engineering, the University of Birmingham, Edgbaston,

Birmingham B15 2TT, UK

* Corresponding author, a.g.shirazi@bham.ac.uk

Abstract

Cold extrusion 3D food printing is an emerging technology which enables the manufacture of food in different shapes and structures and offers huge potential for personalised food products. This study investigates rheological properties and printability (shape fidelity) of food-grade hydrocolloid pastes. From this study, it was found that if the phase angle is in the range of 3° - 15° and the relaxation exponent is in the range of 0.03 -0.13 the paste material is printable, which means that it can support its own-weight if printed. As the demand for inks for 3D printing increases, rheological measurements can rapidly assist with the development of new ink feedstocks.

Keywords: Food 3D printing, Cold extrusion, Rheological Characterization, Phase angle, relaxation exponent

1. Introduction

Additive manufacturing (Truby & Lewis, 2016) often referred to as three-dimensional (3D) printing, enables fabrication of complex structures (Murphy & Atala, 2014). The fabrication process is digitally controlled and the three-dimensional objects are constructed through a layer-by-layer deposition (Chia & Wu, 2015; Guvendiren, Molde, Soares, & Kohn, 2016). This technology has also recently found its way in food applications (Lipton, Cutler, Nigl, Cohen, & Lipson, 2015; Sun, Peng, Yan, H Fuh, & Soon Hong, 2015; Fan Yang, Zhang, & Bhandari, 2017). Among the current 3D printing methods for food applications (Chia & Wu, 2015; Guo & Leu, 2013), extrusion is a prevailing technique because it is easy to develop and it has the broadest set of "inks"(Guvendiren et al., 2016; Tan, Toh, Wong, & Lin, 2018). Inks can be divided into three groups depending on the extrusion techniques (Godoi, Prakash, & Bhandari, 2016): cold extrusion, hot-melt extrusion, and gel-forming extrusion. Both hot-melt and gel-forming extrusion must possess gel-forming mechanisms (Kirchmajer, Gorkin III, & in het Panhuis, 2015; Sun, Zhou, Huang, Fuh, & Hong, 2015). In hot-melt extrusion, semisolid ink is extruded at a relatively high temperature from the nozzle and it needs to solidify almost immediately after extrusion and welds to the previous layer (Sun, Zhou, Yan, Huang, & Lin, 2018). It has been widely applied to create customized 3D chocolate products (Godoi et al., 2016). If the gel-forming mechanism is based on chemical cross-linking the reagents are often harmful and are unlikely to be used for food design. In case of ionotropic cross-linking and complex coacervate formation (Godoi et al., 2016) , the number of edible materials that can be used as inks is limited (Sun et al., 2018) . However, the ink is made of a self-supporting material in cold extrusion and the extrusion is generally conducted at room temperature (Sun et al., 2018).

In order for an ink to be used in cold extrusion-based printing, in general or in food applications for the purpose of this paper, numerous considerations need to be addressed. Besides processing parameters, such as nozzle dimensions, printing speed, extrusion rate (Liu, Zhang, Bhandari, & Wang, 2017; Murphy & Atala, 2014) infill percentage and layer height (Severini, Derossi, & Azzollini, 2016), the ink should display shear thinning behaviour (Ribeiro et al., 2018). This determines if it can be extruded from the nozzle (Ouyang, Highley, Rodell, Sun, & Burdick, 2016). Also, it should be deposited into well-formed geometric shapes without slumping, spreading or bridging (Puttlitz, Stalter, & Faulkner, n.d.). Shape fidelity indicates how much the printed structure is matching the original design. In the case of food materials, the printed structure may go through post-printing process such as

baking for which it is necessary that the printed structure retains its shape (Sun et al., 2018).There is no consensus on approaches to assess or predict shape fidelity, let alone printability (Ribeiro et al., 2018). However, in order to estimate printability (shear thinning and shape fidelity), rheological properties of the material, including viscosity, yield stress, shear moduli and shear recovery should be determined and studied. Although the correlations between the rheological properties of different materials, especially hydrogels, have been studied (Ding & Chang, 2018; Habib, Sathish, Mallik, & Khoda, 2018; Severini, Azzollini, Albenzio, & Derossi, 2018), to date the rheological property or properties and their quantitative limits that dictate 3D printability have not been univocally identified (Kyle, Jessop, Al-Sabah, & Whitaker, 2017).

In one of the earlier reports, Smay *et al* (Smay, Cesarano, Lewis, & Iii, 2002) used concentrated colloidal gels to form self-supporting mesoscale periodic structures. They have reported the minimum ink elasticity required to assemble a given periodic structure. This value was directly related to the ink specific weight.

M´Barki *et al* (M'Barki, Bocquet, & Stevenson, 2017) studied the printability of relatively dense suspensions of Boehmite. They have defined a dimensionless parameter that is a function of material properties (dynamic yield stress, surface tension and density) as well as of printing parameters (nozzle radius and printing height). They have shown that Boehmite inks reach a printed shape fidelity higher than 90% when the defined dimensionless parameter is higher than 1. However, they have determined only a lower limit but not a higher limit for the defined dimensionless number. Kim *et al* (Kim, Bae, & Park, 2017) have selected methyl cellulose at different concentrations as the reference material. They have classified the printability of different methyl cellulose concentrations based on their shear modulus. They have reported that all the materials with a shear modulus higher than 500 Pa can be 3D printed (Table 3) (Kim et al., 2017).

There are several studies that have reported the key role of flow consistency (K) and flow behaviour index (n) in determining the printability. Paxton *et al* (Paxton et al., 2017) have developed a mathematical model and have determined a printability window (printing pressure *vs* needle radius). They have reported that the size of the window of printability is entirely depending on the shear thinning coefficients, K and n (Power-Law model). However, no significant difference between the printability of their samples can be observed, despite considerable difference between their reported flow consistency and flow behaviour indices

and yield stress values (Figure 3, Table 3 and Table 4) (Paxton et al., 2017). Liu et al (Liu, Zhang, Bhandari, & Yang, 2018) studied the 3D printing of mixtures of mashed potato and potato starch. They have concluded that yield stress (τ_0), elastic modulus (G') , K and n (Herschel-Bulkley equation) are the rheological parameters that play an important role in determining the printability. They have reported if $\tau_0 = 312.16\,Pa$, $G' \approx 4000\,Pa$ at the frequency of 1Hz, $K = 118.44\,Pa.s^n$ and $n = 0.63$ the printed objects have good mechanical strength and the material can be easily extruded (Liu et al., 2018).

Vancauwenberghe *et al* (Vancauwenberghe et al., 2017) and Azam *et al* (Azam, Zhang, Bhandari, & Yang, 2018) have identified G' and $\tan\delta$ (where δ is phase angle) as the parameters that play the key role in material printability. Vancauwenberghe *et al* (Vancauwenberghe et al., 2017) assessed the printability of a series of pectin gels by visual observation of the deposition of the material and the 3-D shape stability during and after printing. They reported that if G' was much higher than 1000 Pa and $\tan\delta$ at the frequency of 0.1 rad. s^{-1} was 0.09 then irregular extrusion would happen. If G' was higher than 1000 Pa and $\tan\delta$ at the frequency of 0.1 rad. s^{-1} was 0.21 then the syringe pump would stall automatically. However, when G' was higher than 100 Pa and $\tan\delta$ at the frequency of 0.1 rad. s^{-1} was 0.36, partial spreading happened. Azam *et al* (Azam et al., 2018) studied the 3D printing of the blend of Vitamin D, orange concentrate , wheat starch (15% wt.) and different gums (1% wt.). They have printed three different geometric shapes, hollow cylinder, triangular and square and have evaluated the printability by comparing only the height of the printed objects to the target height in the design. A correlation is observed between their reported rheology and printability results. Their inks containing xanthan gum and guar gum have the same rheological properties ($G'(at\ 1Hz) \approx 6000 - 7000\,Pa$ and $\tan\delta \approx 0.22$). The reported printability for these two inks are almost equal. The best printability that they have obtained is for ink containing κ-carrageenan ($G'(at\ 1Hz) \approx 5000Pa$ and $\tan\delta >$ 0.22).

Lille et al (Lille, Nurmela, Nordlund, Metsä-Kortelainen, & Sozer, 2018) have utilized various protein, starch and fibre-rich food ingredients and their mixtures for 3D printing of ten layers of squares filled with diamond-like structures. They have assessed the printing quality visually and assigned a value of 1(very bad) to 5 (very good) based on the shape-stability of the printed structures. The interesting point in their paper, lies in Table 4. Except one of the formulations (60 % SMP) which was not printable, G', G'' (at the frequency of $0.1Hz$) and the yield stress can be different up to one order of magnitude but their assigned

printability can be the same (10% starch and 35% OPC) . However, the value of their phase angle is not so different. The best printability has been obtained for a formulation with the phase angle of $\approx 11°$ which corresponds to $\tan\delta \approx 0.19$

In this paper, hydrocolloid pastes printability was investigated. It is argued that the phase angle could provide a swift way of assessing the printability of paste materials. This shows that through careful paste design, rheology can be controlled and modified to better suit 3D printing applications.

2. Materials and methods

2.1. Materials

Xanthan gum from Xanthomonas campestris, locust bean gum from Ceratonia siliqua seeds, carrageenan (predominantly κ and lesser amounts of λ carrageenan), pectin (70-75% esterification), agar (congealing temperature <38 °C (1.5% in H_2O)), sodium alginate, guar gum, gum Arabic , gelatin (gel strength 300 bloom), maltodextrin (dextrose equivalent 4.0-7.0), iota-carrageenan (commercial grade, type II) were purchased from Sigma-Aldrich Company Ltd Marketplace (Dorset, UK). Gellan gum, methyl cellulose (viscosity 400 cPs) and lecithin (refined) were purchased from Alfa Aesar Marketplace (Lancaster, UK). Isomalt was a product from MSK specialist food Ingredients. All materials, (non-food grade), were used as received.

2.1.1. Preparation of samples

The hydrocolloid powders were dispersed in deionized water and mixed (L5M, Silverson Machines Ltd., UK) at 10000 rpm for 5 min or longer (until full homogeneity observed) at room temperature. Samples were put in the refrigerator at 4 °C for 48 hr before experiment.

2.2. Methods

2.2.1. Rheology

Rheological characterization of the materials was performed on a Kinexus Rheometer (Pro or Pro+, Malvern panalytical, Malvern, UK) using different geometries (cone and plate, parallel plates sand blasted or serrated, cup and vane) depending to the materials physical state. All measurements were repeated at least three times.

2.2.1.1. Amplitude sweep

In order to determine the linear viscoelastic region, oscillation amplitude sweep (strain controlled) measurements were performed in the range of 0.01-100% at the frequency of 1 Hz at 25 °C (at 20 °C for gelatin samples)

2.2.1.2. Frequency sweep

In order to get the mechanical spectrum of the sample, frequency sweep (at the shear strain of 0.1%) measurements were performed in the range of 10-0.1 Hz at 25 °C (at 20 °C for gelatin samples)

2.2.1.3. Amplitude sweep

In order to measure the yield stress of the samples, oscillation amplitude sweep (strain controlled) measurements were performed in the range of 0.01-100% at the frequency of 1 Hz at 25 °C (at 20 °C for gelatin samples). The yield point was defined as the intersection point between two linear regressions at the plateau-region and viscosity-drop regions of the viscosity-shear stress diagrams, indicating the point at which the material first started to flow.

2.2.1.4. The shear and recovery test

This test comprises of three steps; the first step is a single frequency (1Hz) strain controlled oscillation for 60s , then the sample is exposed to a steady shear rate of 344.8 s^{-1} for 60 s before reverting back to oscillation mode (the same strain value as the first step at 1Hz) to follow structural recovery for 27 min. The measurements were conducted at 25 °C (at 20 °C for gelatin samples)

2.2.2. 3D Printing

A custom built food 3D printing system was used in this study. Printing parameters were adjusted for each sample to get the optimum printability. 3D digital design of cube was generated with the Cura 15.04.6 (Ultimaker B.V., Netherlands). The cubes were printed on a sandpaper (3M™ Utility Cloth Sheet 314D, R.S. Components Limited Marketplace, Corby, UK) at room temperature. For printable materials, three cubes were printed and used for image analysis. Printing time could be as long as 20 min. A 22G needle (inner diameter 0.413 mm) was used for all samples except for agar (4%[1] and 8%) and carrageenan 4%, where an 18G needle (inner diameter 0.838 mm) was used. Moreover for carrageenan 8% and for agar 16% a 2-200 µL pipette tip (inner diameter 0.52 mm) was used because of its conical shape. For all samples a 10 mL syringe was used except for agar (4, 8 and 16%) and carrageenan (4

[1] The numbers in front of the sample names, show the concentration in w/v %.

and 8%) where a 5mL syringe was used. All samples were printed at the flow level (Derossi, Caporizzi, Azzollini, & Severini, 2018) of 40%, however following samples were printed at different flow levels to obtain better printability; carrageenan 2% at 50%, xanthan 4% - gelatin 0.5% at 70%, xanthan 4%-gelatin 2.0% at 55%, guar gum 4% at 50%, agar 4,8 and 16% and carrageenan 4% at 80% and carrageenan 8% at 100 %.

2.2.3. Time-Domain NMR (TD-NMR)

These experiments were conducted using TD-NMR, Minispec 20 Hz, (Bruker BioSpin GmbH, Karlsruhe, Germany). T_2 values were recorded using the software application "t2_cp_mb" a Carr-Purcell-Meiboom-Gill (CPMG) pulse sequence provided by Bruker. For each measurement 200 data points were collected. Pulse separation between the 90° and the 180° pulse was 0.5 ms and the recycle delay was set to 2 s. Data were accumulated with 8 scans. For each measurement sample was placed in a small glass tube and then in an NMR-glass tube (outside diameter 10 mm) at 25 °C. Three samples were prepared and each sample was measured once.

3. Results

Routine rheology measurements were performed to characterise the shear moduli, phase angle within the linear viscoelastic region and yield stress (Supporting information, Table S1). A series of gels were examined and were divided into four groups based on their phase angle value (Table 1).

Table 1 Different groups of hydrocolloids based on their measured phase angle. The numbers in front of the sample names, show the concentration in w/v %.

Phase	δ (°) at	Property	Samples

angle	1 *Hz*		
High	45-90	liquid and non-self-supporting	Gum Arabic (2, 4, 8 and 16%), Isomalt (2, 4, 8 and 16%), Lecithin (2, 4, 8 and 16%), Locust bean (2%), Maltodextrin (2, 4, 8 and 16%), Methylcellulose (2 and 4%), Pectin (2, 4 and 8%), Sodium alginate (2, 4, 8 and 16%)
Medium	15-45	Semisolid but non-self-supporting	Guar gum (2 and 4%), Locust bean (4%), Xanthan (2%, 4%), Xanthan (4%)-Gelatin (0.5%)
Medium-Low	3-15	Semisolid and self-supporting	Agar (2%, 4%, 8% and16%), Carrageenan (2%,4% and 8%), i-Carrageenan (2% and 4%), Gellan (2 and 4%), Xanthan (4%)-Gelatin (1%), Xanthan (4%)-Gelatin (2%), Xanthan (8%), Xanthan (8%)-Gelatin (0.5%), Xanthan (8%)-Gelatin (1%), Xanthan (8%)-Gelatin (2%)
Low	0-3	Hard to extrude	Gelatin (2, 4, 8 and 16%)

All the samples with high phase angle are liquid and non-self-supporting. Samples with low phase angle proved to be too hard to be extruded. Other samples with medium, medium-low and gelatin (2%) (low phase angle) were used to print cubes of 1.5 × 1.5 × 1.5 cm^3 for comparison and characterization. The products were designed to have a cubic shape, however, in practice they did not form perfect cubes and as such were irregularly shaped. The degree of shape irregularity of products from that of a perfect cube was quantified by two parameters; shape inconsistency factor and deformation factor. In order to calculate the shape inconsistency factor, the area of each face of each cube (six area) was measured using image analysis. Each measured area was divided by its theoretical value and the average of the standard deviation of these values multiplied by 100 is defined as shape inconsistency factor (Lipton et al., 2015) (Figure 1). The deformation factor is the ratio of the area of the top to the bottom faces.

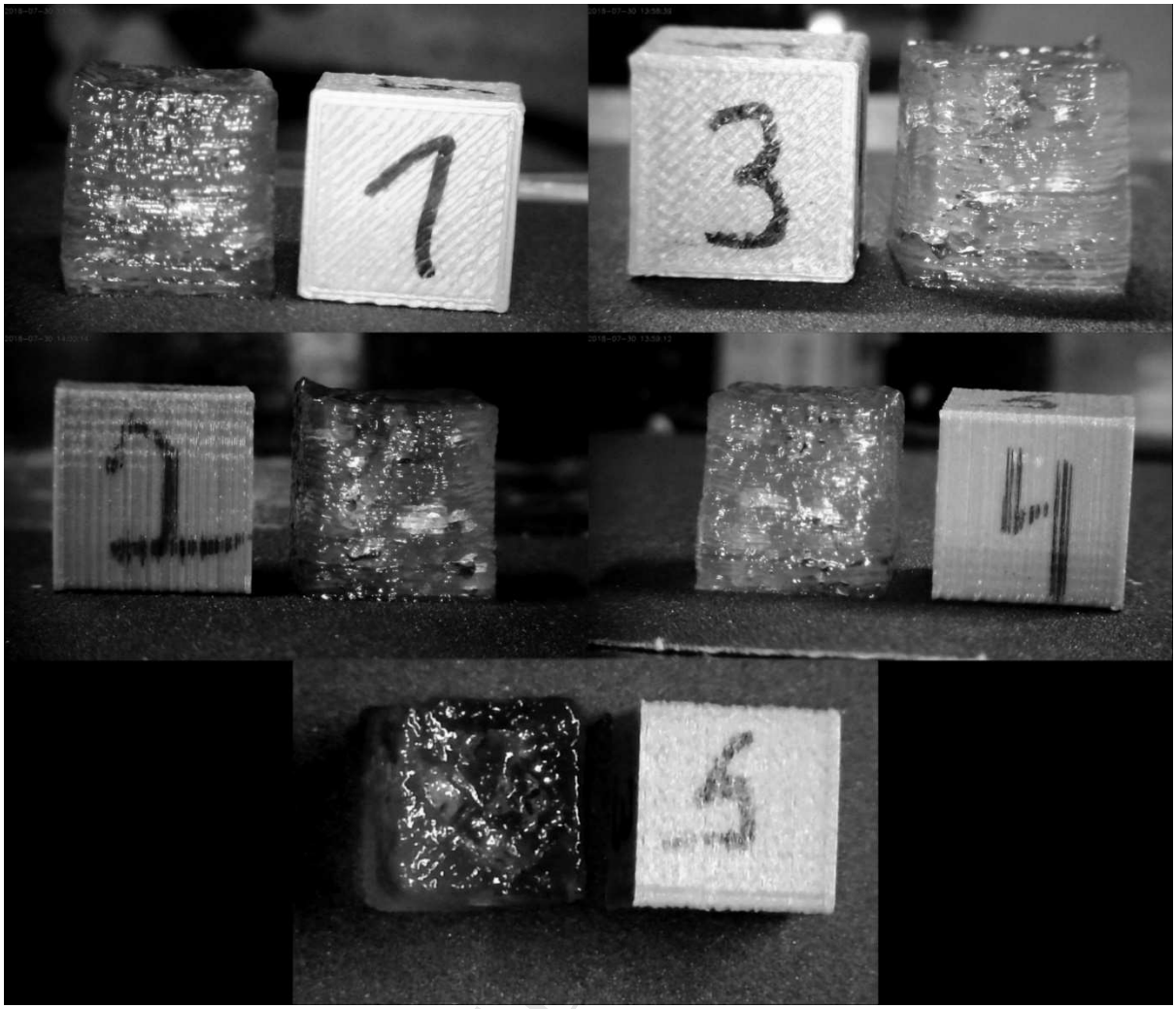

Figure 1 Calculating shape inconsistency factor; the area of each face of each cube (six area) was measured using image analysis. Each measured area was divided by its corresponding value of PLA cube and the average of the standard deviation of these values multiplied by 100 is defined as shape inconsistency factor. The area of the 6th side was calculated from the same image as the 5th area. These images are the printing results for gellan 2%

The results are shown in Figure 2. The image analysis is based on the pictures taken just after printing. The samples were preserved at room temperature overnight and all of them (except guar gum 4%) retained the shape for a few hours. However, their shape change by time was not recorded. For guar gum 2%, locust bean 4%, xanthan 2 and 4% and agar 2%, no defined geometric shape was formed at the end of printing. The samples with the shape inconsistency factor of < 60 and the deformation factor of >0.4 were assigned as printable. An image of printed cubes for each sample is supplied in supporting information (Table S2)

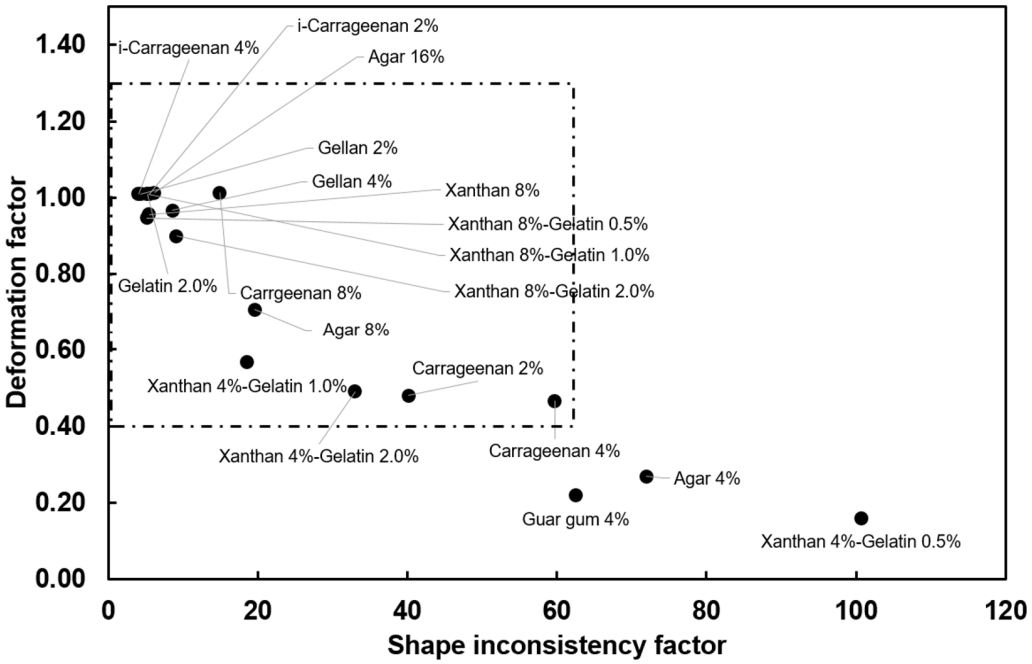

Figure 2 Printability of hydrocolloids with medium, medium-low and low phase angle.

For all the samples, the frequency dependence of G' in the linear viscoelastic region was fitted by a power-law equation ($G' \approx K_1\omega^m$) , where ω is the angular frequency (Martin & Adolf, 1991). The average value of coefficient of determination (R^2) for all samples was higher than 0.94 except for methyl cellulose where it was 0.84. The relaxation exponent, m was calculated and plotted against the phase angle in Figure 3.

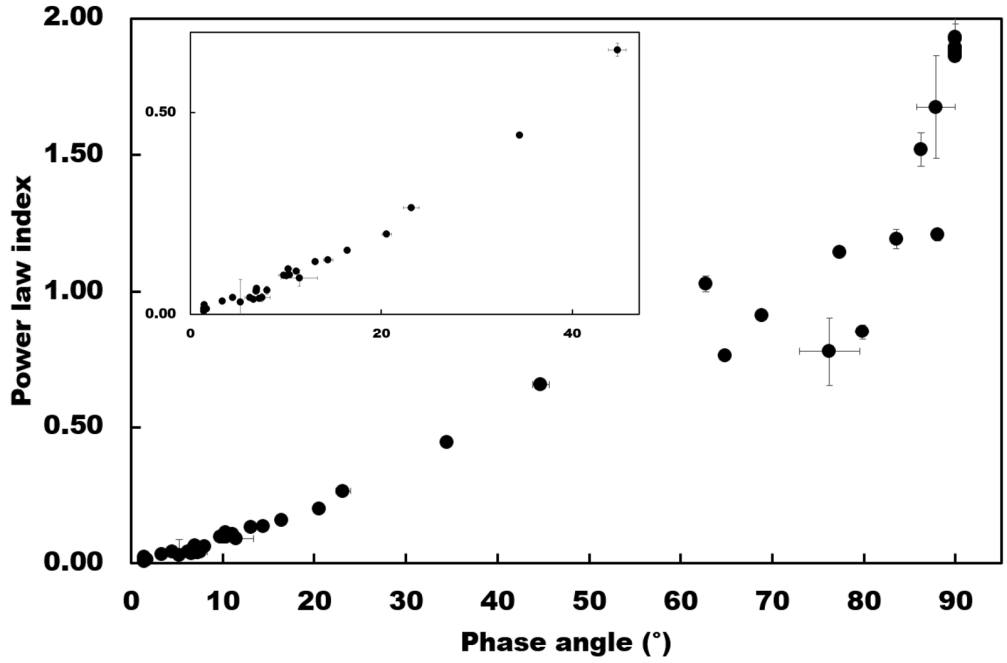

Figure 3 The calculated power law index m in $G' \approx K_1\omega^m$ for different hydrocolloids for the whole range of phase angle (0-90°). The inset shows the corresponding m values for those with phase angle in the range of (0-45°)

A three-step shear rate rheometry test was performed on samples with, medium, medium-low and low phase angle, to evaluate the rate and extent of samples recovery following extrusion. During this process the sample passes from a structured state, to a non-structured state and then it is re-structured to a new state (Abu-Jdayil, 2003). In order to quantify the recovery of the samples after a high shear step, the recovery index was defined as the following

$$Recovery\ index = \frac{\eta_\infty - \eta_{shear}}{\eta_0 - \eta_{shear}} \times 100$$

where $\eta_0$is the initial apparent viscosity at the end of the first step (structured state, low oscillation), and η_∞ is the equilibrium apparent viscosity at the end of the last step (re-structured state, low oscillation). η_{shear} is the apparent viscosity at the end of the high shear step. The graph of recovery index against the phase angle of the sample (re-structured state) is brought in Figure 4. It was not possible to conduct this test for gelatin samples, because samples were ejected out of the geometry during the high shear step.

T_2 (spin–spin relaxation time) was also recorded as an indicator for gel strength and water binding strength and the results are presented in Figure 5.

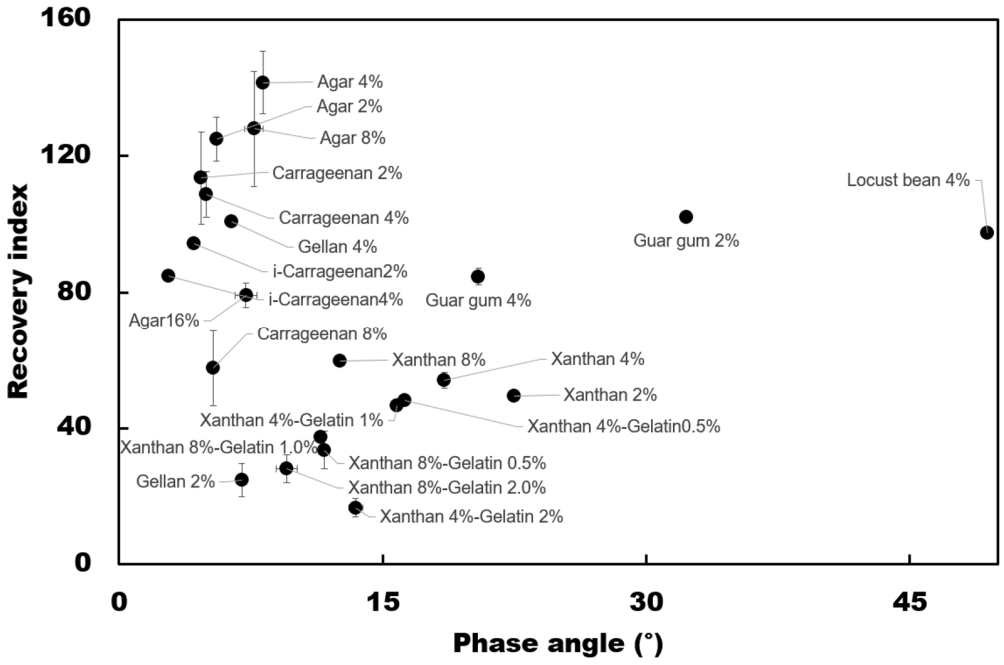

Figure 4 Recovery index vs phase angle for the re-structured sample

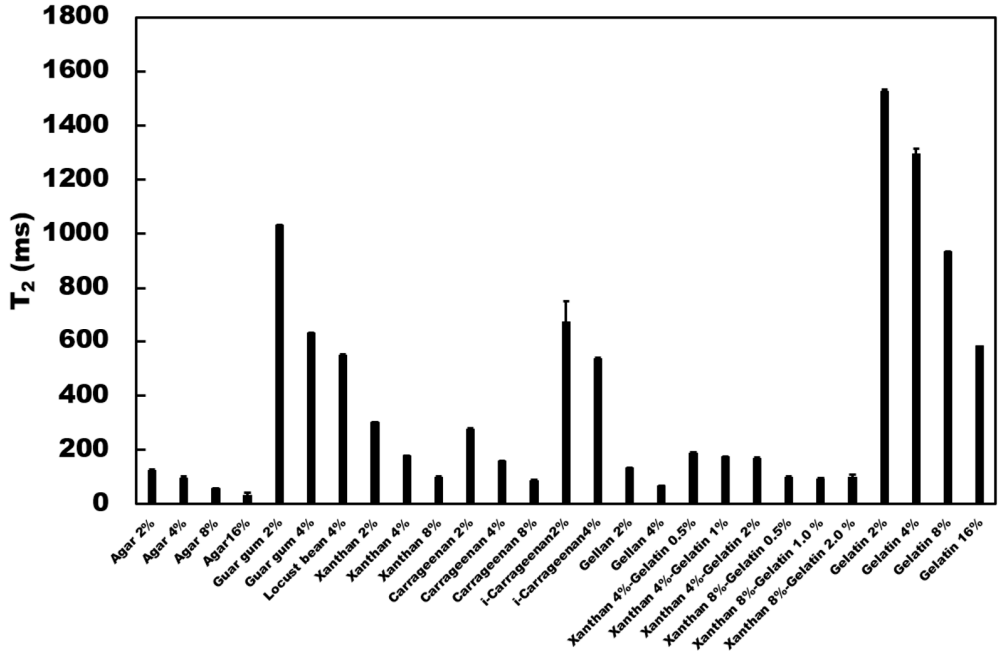

Figure 5 Relaxation time as indicator for gel strength and water binding strength of hydrocolloid samples measured by NMR analysis

4. Discussion

Yield stress materials encompass a broad range of materials from colloidal assemblies and gels to emulsions and non-Brownian suspensions (Bonn, Denn, Berthier, Divoux, & Manneville, 2017). Each of these materials appears capable of flowing only when a sufficiently large stress has been applied to it (Baudez & Coussot, 2004). A gel is an intermediate between a solid and liquid possessing both elastic (solid) and viscous (liquid) characteristics (Nazir, Asghar, & Aslam Maan, 2017). Soft gels, including simple water based gels, can be considered as simple physical models for foods (Vilgis, 2015). For a few of the polysaccharides, after being dispersed in water and after complete hydration, the polymer strands are cross-linked. Beyond a certain concentration (packing fraction), the dispersion turns into a gel (jammed systems) (Bonn et al., 2017; Conrad et al., 2011; Nazir et al., 2017).

To function properly as 3D printing ink, the sample must combine liquid-like characteristics to flow under the shear in the extruder and solid-like characteristics to form a self-supporting structure once the applied shear is removed. Pasty materials (gels) are capable of flowing only when a sufficiently large stress has been applied to it, a characteristic feature associated with their ‘‘jammed’’ structure (Baudez & Coussot, 2004).

The phase angle (or loss angle) is the inverse tangent of viscous modulus to the elastic modulus (G''/G')(Coussot, 2005). Generally, the phase angle, δ lies between 0° (purely elastic, solid) and 90° (purely viscous, liquid)(Schultz & Struble, 1993). For gels 1.2° < δ < 64° (Dong & Lakes, 2012) and for elasticity dominant gel-like structures δ is less than 45° (Lille et al., 2018). The phase angle below 10 ° in the linear viscoelastic region is characteristic of viscoelastic solids (Patel, Cludts, Sintang, Lesaffer, & Dewettinck, 2014).

Here, Figure 2, we have shown that if the phase angle of the shear thinning sample is in the medium -low range, it will be self-supporting and extrudable. The same factors that give rise to syneresis in carrageenan and agar, interfere in printing as well. By using low flow levels (Derossi et al., 2018) or narrow needles only the aqueous phase goes out of the syringe but not solid material. The flow level that was used to print agar and carrageenan samples is twice that of used for printing iota-carrageenan. This may be one reason for their low printability. Although for agar, two batches were used (with the same catalogue number from the same supplier). They had very different colours (white and beige), for agar 2 and 4% the phase angles were very different for the two batches (70.78 ± 2.39 and 33.88 ± 2.47 for white coloured sample and 5.25 ± 0.16 and 7.24 ± 0.27 for the beige coloured sample). Other parameters (shear banding or radial viscous fingering (Philippe Coussot, Personal communication) are likely involved in the rheology of agar (and carrageenan) samples that lead to non-realistic phase angle values.

For the medium phase angle samples, the yield stress changes over four orders of magnitude and G' changes over three orders of magnitude. However, none of them proved to be printable into self-supporting structures. For medium-low range of phase angle, yield stress mainly varies in the range of 1-150 Pa and G' is in the range of 150-40000 Pa, which overlay those of medium phase angle range. But the latter shows some degrees of shape fidelity. However, the former does not form any finite geometric shape. Moreover, no correlation between elastic shear modulus, yield stress and shape inconsistency or deformation factor was observed (Supporting information, Figure S1).

For gels, in the linear viscoelastic region, G' (and G'') can be represented by a power law function of angular frequency ($G' \approx K_1\omega^m$) (Kavanagh & Ross-Murphy, 1998). The exponent, m , should have some value between 0 (typical elastomeric solid) and 2 (ideal) (Muller, Gérard, Dugand, Rempp, & Gnanou, 1991). A notable feature of m, is that it varies among different materials and continuously but rather weakly for a single material type

depending on its formulation (for example its solid fraction) (Chen, Wen, Janmey, Crocker, & Yodh, 2010; Muller et al., 1991). Here, it has been shown that if 0.03 < m <0.13, the material can support its own weight (Figure 2). A question might arise that m for agar (2 and 4%) is 0.03 but they proved to be non-printable. As it was explained earlier it is very likely that some instabilities are involved in agar rheology experiments (Gonuguntla, Sharma, & Subramanian, 2006). Even so, it does not contradict our design rule. Because the m value for agar 2 and 4% (0.03) lies over the lower extreme of this range.

Therefore, the dependence of G' and G'' on frequency (mechanical spectrum) can be used to characterize viscoelastic properties (Brummer, 2006) or to classify the dispersion (Morris, Nishinari, & Rinaudo, 2012). If G' and G'' are weakly dependent to the frequency and G' is considerably higher than G'' , the gel is considered as self-supporting , demouldable, strong or true gel (Kasapis & Bannikova, 2016; Morris et al., 2012). Among medium and medium – low phase angle samples, only guar gum (2 and 4%) and locust bean (4%) are not "true gels". In the mechanical spectrum (Supporting information, Figure S2) for guar gum 2%, a cross-over of G' and G'' can be observed at the frequency of ~ 0.2 Hz. However, for guar gum 4%, no cross-over observed in the range of 0.1-10 Hz ($G' > G''$), but it is seen that it can occur below 0.1 Hz. For locust bean 4%, a cross-over is observed at the frequency of ~ 1.3 Hz. If the curves of G' and G'' pass a cross-over point, the sample is categorized under a semi-dilute solution of entangled polymer coils (Morris et al., 2012). Based on these definitions, among medium and medium –low phase angle samples, only guar gum (2 and 4%) and locust bean (4%) are not "true gels". However, being a "true gel" cannot be interpreted as being printable or self-supportive. Agar (4%), xanthan (2% and 4%) and xanthan 4%-gelatin 0.5% are true gels but they are proved to not to be able to retain the shape.

Pastes are thixotropic fluids, which means that they show shear thinning behaviour combined with a time dependency. Their viscosity drops when subjected to a constant shear rate for a period of time, but it recovers substantially over a period of time after the shearing forces have been removed (Coussot, 2005, 2007). The major difference between colloidal systems and polymeric liquids is that polymer solutions have much higher elastic recovery than colloidal systems. Due to short range of interparticle forces, colloidal dispersions show less elastic recovery (Russel, Saville, & Schowalter, 1989). Here, the recovery of the samples after being subjected to a shear rate of 344.90 s^{-1} was evaluated. It is the shear rate that 10 ml of a non-Newtonian fluid with the flow behaviour index of 0.1 is subjected to when passing through a tube with a diameter of 1 mm during 2min.

All samples' viscosity decreased significantly at high shear rate and recovered rapidly at low shear rate, and quickly reached a stabilized state. The thixotropic behaviour for two of the samples, as an example, is shown in Figure S3. The mechanism of gelation of food hydrocolloids are well-studied (Banerjee & Bhattacharya, 2012). For example, the mechanism of gelation of κ-carrageenan is reported as a process divided into several stages; starting from random coil conformation to the formation of a helical dimer and finally to aggregation of helical dimers, upon increasing the concentration (Tecante & Nez Santiago, 2012). The recovery index is lower than 100 for most of the samples. It shows that the equilibrium configuration after restructuring is different than that of before breakage as a result of the shear. Khabaz et *al.*(Khabaz, Liu, Cloitre, & Bonnecaze, 2017), using computational simulations, have shown that the microstructure and shear rheology of highly concentrated, jammed suspensions of soft particles depends on polydispersity and shear rate and glassy suspensions with a low degree of polydispersity evolve to face-centred cubic and hexagonal close-packed structures at low and high shear rates, respectively. However, these soft matter systems are diverse structurally, highly complex rheologically and contain hierarchical structures in a wide range of macro- to nano-scale (Stokes & Frith, 2008). Moreover, experimental complications, such as shear banding, non-uniform deformation might arise during rheology measurement (Coussot, 2007; Stokes & Frith, 2008).

It is observed, Figure 4, that the phase angle (a function of G''/G') plays a more important role than the recovery index in determining the printability of the sample. It is seen that guar gum 4% and locust bean 4% are recovered as 80 and 100%. However, they are not printable. Gellan 2% has a very low recovery index, but a very high printability.

The gel- and water binding strength of the hydrocolloid samples was investigated by NMR analysis. The value of the relaxation time (T_2) was used as indicator for water binding capacity and gel strength. A small T_2 indicates a small degree of moisture freedom in the sample and strong binding with solid components. While a large T_2 indicates a large degree of moisture freedom (Fanli Yang, Zhang, Bhandari, & Liu, 2018). A seen in Figure 5, these samples show very different of gel strength and water binding. However, no direct relationship is observed with their printability. Gellan 2% and iota-carrageenan 2% have very similar printability but their T_2 are very different. There is very weak interaction between gelatin samples and water compared to other samples. But they proved to be very hard to extrude and only gelatin (2%) was printable.

5. Conclusion

The viscoelastic behaviour (rheological properties as well as thixotropic behaviour) and the printability of food grade hydrocolloid pastes were investigated in this study. The results from the study shows that the phase angle and the relaxation exponent could be used to understand the solid and liquid characteristic of the paste behaviour during the cold extrusion 3D printing process. The results show that if $3° < \delta < 15°$ and $0.03 < m < 0.13$, the ink is self-supporting. Since measuring phase angle in the viscoelastic region is straight forward, the phase angle could be used as quick and effective means of studying the printability of the formulation. The obtained knowledge can be used as a design rule for food (hydrocolloids) printing processes to develop new feedstocks for food 3D printing.

Acknowledgement

The authors would like to acknowledge John Duffy from Malvern Panalytical for his helpful discussion. This work was supported by the Engineering and Physical Sciences Research Council [grant number EP/N024818/1].

References

Abu-Jdayil, B. (2003). Modelling the time dependent rheological behavior of semisolid foodstuffs. *Journal of Food Engineering*, *57*(1), 97–102. https://doi.org/10.1016/S0260-8774(02)00277-7

Azam, R. S. M., Zhang, M., Bhandari, B., & Yang, C. (2018). Effect of Different Gums on Features of 3D Printed Object Based on Vitamin-D Enriched Orange Concentrate. *Food Biophysics*, 1–13. https://doi.org/10.1007/s11483-018-9531-x

Banerjee, S., & Bhattacharya, S. (2012). Food Gels: Gelling Process and New Applications. *Critical Reviews in Food Science and Nutrition*, *52*(4), 334–346. https://doi.org/10.1080/10408398.2010.500234

Baudez, J. C., & Coussot, P. (2004). Abrupt transition from viscoelastic solidlike to liquidlike behavior in jammed materials. *Physical Review Letters*, *93*(12), 1–4. https://doi.org/10.1103/PhysRevLett.93.128302

Bonn, D., Denn, M. M., Berthier, L., Divoux, T., & Manneville, S. (2017). Yield stress materials in soft condensed matter. *Reviews of Modern Physics*, *89*(3), 1–40. https://doi.org/10.1103/RevModPhys.89.035005

Brummer, R. (2006). *Rheology Essentials of Cosmetic and Food Emulsions*. Berlin/Heidelberg: Springer-Verlag. https://doi.org/10.1007/3-540-29087-7

Chen, D. T. N., Wen, Q., Janmey, P. A., Crocker, J. C., & Yodh, A. G. (2010). Rheology of Soft Materials. *Annual Review of Condensed Matter Physics*, *1*(1), 301–322. https://doi.org/10.1146/annurev-conmatphys-070909-104120

Chia, H. N., & Wu, B. M. (2015). Recent advances in 3D printing of biomaterials. *Journal of Biological Engineering*, *9*, 4. https://doi.org/10.1186/s13036-015-0001-4

Conrad, J. C., Ferreira, S. R., Yoshikawa, J., Shepherd, R. F., Ahn, B. Y., & Lewis, J. A. (2011). Designing colloidal suspensions for directed materials assembly. *Current Opinion in Colloid and Interface Science*, *16*(1), 71–79. https://doi.org/10.1016/j.cocis.2010.11.002

Coussot, P. (2005). *Rheometry of Pastes, Suspensions,and Granular Materials*. *ED. Wiley-Interscience*.

Coussot, P. (2007). Rheophysics of pastes: a review of microscopic modelling approaches. *Soft Matter*, *3*(5), 528. https://doi.org/10.1039/b611021p

Derossi, A., Caporizzi, R., Azzollini, D., & Severini, C. (2018). Application of 3D printing for customized food. A case on the development of a fruit-based snack for children. *Journal of Food Engineering*, *220*, 65–75. https://doi.org/10.1016/j.jfoodeng.2017.05.015

Ding, H., & Chang, R. (2018). Printability Study of Bioprinted Tubular Structures Using Liquid Hydrogel Precursors in a Support Bath. *Applied Sciences*, *8*(3), 403. https://doi.org/10.3390/app8030403

Dong, L., & Lakes, R. S. (2012). Advanced damper with negative structural stiffness elements. *Smart Materials and Structures*, *21*(7), 075026. https://doi.org/10.1088/0964-1726/21/7/075026

Godoi, F. C., Prakash, S., & Bhandari, B. R. (2016). 3d printing technologies applied for food design: Status and prospects. *Journal of Food Engineering*, *179*, 44–54. https://doi.org/10.1016/j.jfoodeng.2016.01.025

Gonuguntla, M., Sharma, A., & Subramanian, S. A. (2006). Elastic Contact Induced Self-Organized Patterning of Hydrogel Films. *Macromolecules*, *39*(9), 3365–3368. https://doi.org/10.1021/ma0600411

Guo, N., & Leu, M. C. (2013). Additive manufacturing: Technology, applications and research needs. *Frontiers of Mechanical Engineering*, *8*(3), 215–243. https://doi.org/10.1007/s11465-013-0248-8

Guvendiren, M., Molde, J., Soares, R. M. D., & Kohn, J. (2016). Designing Biomaterials for 3D Printing. *ACS Biomaterials Science and Engineering*, *2*(10), 1679–1693. https://doi.org/10.1021/acsbiomaterials.6b00121

Habib, A., Sathish, V., Mallik, S., & Khoda, B. (2018). 3D printability of alginate-carboxymethyl cellulose hydrogel. *Materials*, *11*(3). https://doi.org/10.3390/ma11030454

Kasapis, S., & Bannikova, A. (2016). *Rheology and Food Microstructure*. *Advances in Food Rheology and Its Applications*. Elsevier Ltd. https://doi.org/10.1016/B978-0-08-100431-9.00002-4

Kavanagh, G. M., & Ross-Murphy, S. B. (1998). Rheological characterisation of polymer gels. *Progress in Polymer Science (Oxford)*, *23*(3), 533–562. https://doi.org/10.1016/S0079-6700(97)00047-6

Khabaz, F., Liu, T., Cloitre, M., & Bonnecaze, R. T. (2017). Shear-induced ordering and crystallization of jammed suspensions of soft particles glasses. *Physical Review Fluids*, *2*(9), 093301. https://doi.org/10.1103/PhysRevFluids.2.093301

Kim, H. W., Bae, H., & Park, H. J. (2017). Classification of the printability of selected food for 3D printing: Development of an assessment method using hydrocolloids as reference material. *Journal of Food Engineering*, *215*, 23–32. https://doi.org/10.1016/j.jfoodeng.2017.07.017

Kirchmajer, D. M., Gorkin III, R., & in het Panhuis, M. (2015). An overview of the suitability of hydrogel-forming polymers for extrusion-based 3D-printing. *J. Mater. Chem. B*, *3*(20), 4105–4117. https://doi.org/10.1039/C5TB00393H

Kyle, S., Jessop, Z. M., Al-Sabah, A., & Whitaker, I. S. (2017). 'Printability'' of Candidate Biomaterials for Extrusion Based 3D Printing: State-of-the-Art.' *Advanced Healthcare Materials*, *6*(16), 1700264. https://doi.org/10.1002/adhm.201700264

Lille, M., Nurmela, A., Nordlund, E., Metsä-Kortelainen, S., & Sozer, N. (2018). Applicability of protein and fiber-rich food materials in extrusion-based 3D printing. *Journal of Food Engineering*, *220*, 20–27. https://doi.org/10.1016/j.jfoodeng.2017.04.034

Lipton, J. I., Cutler, M., Nigl, F., Cohen, D., & Lipson, H. (2015). Additive Manufacturing for the Food Industry - A review. *Trends in Food Science & Technology*, *43*(1), 114–123. https://doi.org/10.1016/j.tifs.2015.02.004

Liu, Z., Zhang, M., Bhandari, B., & Wang, Y. (2017). 3D printing: Printing precision and application in food sector. *Trends in Food Science and Technology*, *69*, 83–94. https://doi.org/10.1016/j.tifs.2017.08.018

Liu, Z., Zhang, M., Bhandari, B., & Yang, C. (2018). Impact of rheological properties of mashed potatoes on 3D printing. *Journal of Food Engineering*, *220*, 76–82. https://doi.org/10.1016/j.jfoodeng.2017.04.017

M'Barki, A., Bocquet, L., & Stevenson, A. (2017). Linking Rheology and Printability for Dense and Strong Ceramics by Direct Ink Writing. *Scientific Reports*, *7*(1), 6017. https://doi.org/10.1038/s41598-017-06115-0

Martin, J. E., & Adolf, D. (1991). The Sol-Gel Transition in Chemical Gels. *Annual Review of Physical Chemistry*, *42*(1), 311–339. https://doi.org/10.1146/annurev.pc.42.100191.001523

Morris, E. R., Nishinari, K., & Rinaudo, M. (2012). Gelation of gellan - A review. *Food Hydrocolloids*, *28*(2), 373–411. https://doi.org/10.1016/j.foodhyd.2012.01.004

Muller, R., Gérard, E., Dugand, P., Rempp, P., & Gnanou, Y. (1991). Rheological Characterization of the Gel Point: A New Interpretation. *Macromolecules*, *24*(6), 1321–1326. https://doi.org/10.1021/ma00006a017

Murphy, S. V., & Atala, A. (2014). 3D bioprinting of tissues and organs. *Nature Biotechnology*, *32*(8), 773–785.

https://doi.org/10.1038/nbt.2958

Nazir, A., Asghar, A., & Aslam Maan, A. (2017). *Chapter 13 - Food Gels: Gelling Process and New Applications A2 - Ahmed, J. Advances in Food Rheology and Its Applications*. Elsevier Ltd. https://doi.org/https://doi.org/10.1016/B978-0-08-100431-9.00013-9

Ouyang, L., Highley, C. B., Rodell, C. B., Sun, W., & Burdick, J. A. (2016). 3D Printing of Shear-Thinning Hyaluronic Acid Hydrogels with Secondary Cross-Linking. *ACS Biomaterials Science and Engineering*, *2*(10), 1743–1751. https://doi.org/10.1021/acsbiomaterials.6b00158

Patel, A. R., Cludts, N., Sintang, M. D. Bin, Lesaffer, A., & Dewettinck, K. (2014). Edible oleogels based on water soluble food polymers: preparation, characterization and potential application. *Food & Function*, *5*(11), 2833–2841. https://doi.org/10.1039/c4fo00624k

Paxton, N., Smolan, W., Böck, T., Melchels, F., Groll, J., & Jungst, T. (2017). Proposal to assess printability of bioinks for extrusion-based bioprinting and evaluation of rheological properties governing bioprintability. *Biofabrication*, *9*(4), 044107. https://doi.org/10.1088/1758-5090/aa8dd8

Puttlitz, K., Stalter, K., & Faulkner, L. (n.d.). *Handbook of Lead-Free Solder Technology for Microelectronic Assemblies.* Boca Raton: CRC Press.

Ribeiro, A., Blokzijl, M. M., Levato, R., Visser, C. W., Castilho, M., Hennink, W. E., … Malda, J. (2018). Assessing bioink shape fidelity to aid material development in 3D bioprinting. *Biofabrication*, *10*(1). https://doi.org/10.1088/1758-5090/aa90e2

Russel, W. B., Saville, D. A., & Schowalter, W. R. (1989). A Survey of Colloidal Dispersions. *Colloidal Dispersions*, 1–20. https://doi.org/10.1017/CBO9780511608810.004

Schultz, M. A., & Struble, L. J. (1993). Use of oscillatory shear to study flow behavior of fresh cement paste. *Cement and Concrete Research*, *23*(2), 273–282. https://doi.org/10.1016/0008-8846(93)90092-N

Severini, C., Azzollini, D., Albenzio, M., & Derossi, A. (2018). On printability, quality and nutritional properties of 3D printed cereal based snacks enriched with edible insects. *Food Research International*, *106*(January), 666–676. https://doi.org/10.1016/j.foodres.2018.01.034

Severini, C., Derossi, A., & Azzollini, D. (2016). Variables affecting the printability of foods: Preliminary tests on cereal-based products. *Innovative Food Science and Emerging Technologies*, *38*, 281–291. https://doi.org/10.1016/j.ifset.2016.10.001

Smay, J. E., Cesarano, J., Lewis, J. A., & Iii, J. C. (2002). Colloidal inks for directed assembly of 3-D periodic structures. *Langmuir*, *18*(14), 5429–5437. https://doi.org/10.1021/la0257135

Stokes, J. R., & Frith, W. J. (2008). Rheology of gelling and yielding soft matter systems. *Soft Matter*, *4*(6), 1133–1140. https://doi.org/10.1039/b719677f

Sun, J., Peng, Z., Yan, L., H Fuh, J. Y., & Soon Hong, G. (2015). 3D food printing—An innovative way of mass customization in food fabrication. *Journal of Bioprinting*, *1*(1), 27–38. https://doi.org/10.18063/IJB.2015.01.006

Sun, J., Zhou, W., Huang, D., Fuh, J. Y. H., & Hong, G. S. (2015). An Overview of 3D Printing Technologies for Food Fabrication. *Food and Bioprocess Technology*, *8*(8), 1605–1615. https://doi.org/10.1007/s11947-015-1528-6

Sun, J., Zhou, W., Yan, L., Huang, D., & Lin, L. ya. (2018). Extrusion-based food printing for digitalized food design and nutrition control. *Journal of Food Engineering*, *220*, 1–11. https://doi.org/10.1016/j.jfoodeng.2017.02.028

Tan, C., Toh, W. Y., Wong, G., & Lin, L. (2018). Extrusion-based 3D food printing – Materials and machines. *International Journal of Bioprinting*, *4*(2), 1–13. https://doi.org/10.18063/ijb.v4i2.143

Tecante, A., & Nez Santiago, M. del C. (2012). Solution Properties of κ-Carrageenan and Its Interaction with Other Polysaccharides in Aqueous Media. *Rheology*. https://doi.org/10.5772/36619

Truby, R. L., & Lewis, J. A. (2016). Printing soft matter in three dimensions. *Nature*, *540*(7633), 371–378. https://doi.org/10.1038/nature21003

Vancauwenberghe, V., Katalagarianakis, L., Wang, Z., Meerts, M., Hertog, M., Verboven, P., … Nicolaï, B. (2017). Pectin based food-ink formulations for 3-D printing of customizable porous food simulants. *Innovative Food Science and Emerging Technologies*, *42*(July 2016), 138–150. https://doi.org/10.1016/j.ifset.2017.06.011

Vilgis, T. A. (2015). Gels: Model systems for soft matter food physics. *Current Opinion in Food Science*, *3*, 71–84. https://doi.org/10.1016/j.cofs.2015.05.009

Yang, F., Zhang, M., & Bhandari, B. (2017). Recent development in 3D food printing. *Critical Reviews in Food Science and Nutrition*, *57*(14), 3145–3153. https://doi.org/10.1080/10408398.2015.1094732

Yang, F., Zhang, M., Bhandari, B., & Liu, Y. (2018). Investigation on lemon juice gel as food material for 3D printing and optimization of printing parameters. *LWT - Food Science and Technology*, *87*, 67–76. https://doi.org/10.1016/j.lwt.2017.08.054

Highlights

- 3D printing of hydrocolloids is influenced by their rheological properties
- Thixotropic hydrocolloid systems were used as a model for food 3D printing
- Over 50 combinations (concentration/type) of hydrocolloids were analysed and their shear moduli, viscosities and the relaxation parameters were reported
- Phase angle and relaxation exponent are used to get insight on 3D printing of hydrocolloids
- This design rule can be used to identify food formulations with tailored made properties for use in food 3D printing